

Evidence for Material Removal and/or Subsidence of the Martian Lithosphere from a Global Dataset of Surface Faults. L. L. Dimitrova¹, W. E. Holt¹, A. J. Haines² and R. A. Schultz³, ¹Department of Geosciences, Stony Brook University, Stony Brook, NY 11794 (Lada.Dimitrova@stonybrook.edu, William.Holt@stonybrook.edu), ²Department of Earth Sciences, University of Cambridge, UK (ajh50@cam.ac.uk), ³Department of Geological Sciences and Engineering, University of Nevada, Reno, NV (schultz@mines.unr.edu).

Introduction: Two different models of the lithospheric stress have been employed to explain the majority of the faulting in and around Tharsis. The model of [1] is dominated by the flexural response to a Tharsis load. The model of [2] is based on stresses associated with gravitational potential energy (GPE) differences as derived by the topography model of [3] and crustal thickness model of [4]. Both [1] and [2] predict the radial grabens in the southern part of the periphery of Tharsis. Model [1] fails to fit the normal faults in the center of Tharsis, although it does have an improved fit to the normal faults extending north and north-east of Alba Patera. The GPE model fits ~70% of the normal faults in Tharsis. This fit implies that possibly the normal faults in and around Tharsis formed early in the Martian history when elastic thicknesses as well as membrane and flexural stresses were small, and viscous rather than elastic processes dominated.

The studies of [1, 2] were biased towards the normal faults in the western hemisphere due to the available data set. Recent orbital exploration has led to the creation of expanded fault data sets [5, 6].

In [7, this volume, Fig. 1] we estimated the misfit of the GPE associated model with the strain from Kostrov summation for the normal and reverse faults of [5]. The normal faults mapped to-date are clustered in the western hemisphere around Tharsis, and hence, are (1) well fitted by the GPE model and (2) provide little to no constraint on processes elsewhere. On the other hand, the reverse faults are much more uniformly distributed and provide better constraints; in particular, reverse faults in high topography areas are ill-fitted by the GPE model.

The GPE model assumes that (1) present-day topography is the paleotopography, (2) present-day crustal thickness is the paleo-crustal thickness, (3) uniform crustal and mantle densities of 2900 kg/m³ and 3500 kg/m³ respectively consistent with [4]. Thus, we consider if small perturbations in GPE or membrane stresses might explain the misfit to the faults. Perturbations in membrane stresses will manifest predominantly as a topography changes since the time of faulting. Perturbations in GPE related stresses will manifest predominantly in crustal thickness changes since the time of faulting or lateral crust and mantle density variations.

Methodology: We perform inversions minimizing the surface integral of the misfit for additional stresses due to GPE variations or membrane displacements. To

do this we use a forward thin-sheet model [9] to calculate the Green's function responses to forcing terms of spherical harmonics degree and order 17. We invert for the coefficients for these Green's functions responses such that the resultant stress field, when added to the GPE stress field, minimizes the surface integral of the misfit. We sum the spherical harmonics weighted by these coefficients to calculate the corresponding membrane displacements or GPE changes. The GPE variations are interpreted in end-member cases as density variations and Moho depth variations.

Results: *Inversion for membrane displacement.* For a given spherical degree and order cut-off, the stresses associated with membrane displacement fit the normal faults slightly worse than the stresses with additional GPE (Fig. 1, also [8]); the majority of the misfit is north-northeast of Alba Patera. The membrane displacement model fails to improve the fit to the reverse faults even for spherical degree and order 17 cut-off. The major area of improvement is to the wrinkle ridges in Lunae Planum, and to a lesser degree to reverse faults just north-northeast and south-southwest of Hellas Planitia. The membrane displacements are within ± 472 m.

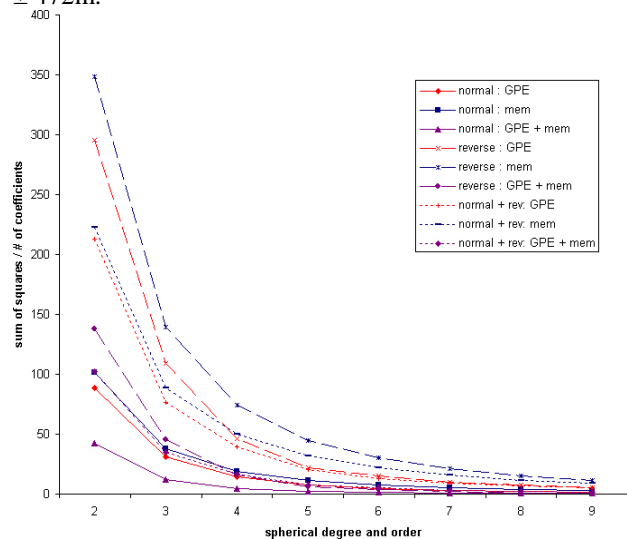


Figure 1 Sum of squares per number of coefficients for our inversions to degree and order 9. Results for GPE stress alone inversions are shown in red, for membrane stress alone in blue, and for both GPE and membrane stress in purple. The inversion to the normal faults alone are in solid, the reverse faults alone are in long dashes, and both the normal and reverse faults in short dashes.

Inversion for additional GPE or both GPE and membrane displacement. Stresses associated with perturbations to GPE, or perturbations to both GPE and membrane sources, do improve the fit to many of the faults (Fig. 1, also [8]). For the normal faults, the improvement is north/north-east of Alba Patera and north/northeast portion of Arabia Terra, while minor improvement is seen in the vicinity of Elysium Mons (Fig. 2A). For the reverse faults, significant improvement is seen for the “classical” wrinkle ridges in Solis and Lunae Plana, while some improvement is seen in Sirenum and Cimmeria Terrae and in the highlands surrounding Hellas Planitia (Fig. 2A).

Models with additional variation in both GPE and small membrane displacements (± 175 m) provide the best fit. Inversion results for both normal and reverse faults show correlated changes in GPE and membrane displacements, requiring additional GPE and/or upward vertical displacement under Tharsis and Margaritifer Terra and Meridiani Planum in the western hemisphere and Hellas and Utopia Planitia in the eastern hemisphere (Fig. 2B,C). While the results for Tharsis may

reflect deviations from the average crustal density as proposed by [4], which will significantly affect the base GPE model, the remaining areas can be explained by a combination of removal of material and subsidence after the fault formation. This interpretation is also consistent with these areas associated with very large craters and/or networks of outflow channels. Alternatively, the variations in GPE may be due to lateral density variations on the order of $\pm 69 \text{ kg.m}^{-3}$ for the crust, $\pm 161 \text{ kg.m}^{-3}$ for the mantle, $\pm 35 \text{ kg.m}^{-3}$ for both the crust and the mantle. These density differences are only a few percent and will not affect the gravity field significantly.

References: [1] Banerdt & Golombek M. (2000) *LPS XXXI*, Abstract #2038. [2] Dimitrova et al. (2006) *GRL* 33, L08202. [3] Zuber M.T. et al. (2000) *Science*, 287, 1788–1793. [4] Neumann G.A. et al. (2004) doi:10.1029/2004JE002262. [5] Knapmeyer et al. (2006) *JGR* 111, E11006. [6] Anderson et al. (2006) *LPS XXXVII*, Abstract #1883 [7] Dimitrova et al. (2008) *LPS XXXIX*, Abstract #1848 [8] Dimitrova et al (2007) *7th Intl. Conf. On Mars*, Abstract #3337. [9] Flesch et al. (2001) *JGR* 106, 16435-16460.

Figure 2. A) The misfit to all the faults of the combined GPE and membrane inversion of degree 5. The corresponding vertical deflections B) and GPE perturbations C).

